Composition Dependence of the Superconducting Properties of UTe2

Composition Dependence of the Superconducting Properties of UTe_2

Luke Pritchard Cairns, Callum R. Stevens, Christopher D. O'Neill, and Andrew Huxley
School of Physics and Astronomy and CSEC, University of Edinburgh, Edinburgh, EH9 3FD, UK
(Dated: June 9, 2020)

A better understanding of the synthesis conditions, composition and physical properties of UTe_2 are required to interpret previously reported unconventional superconductivity. Here we report how the superconducting properties of single crystals depend on the ratio of elements present in their synthesis by chemical vapour transport. We have obtained crystals with the highest reported ambient pressure T_c and a larger superconducting heat capacity jump from a growth with a U:Te ratio different from that widely used in the literature. For these crystals, the ratio of residual heat capacity in the superconducting state to that of the normal state, γ^*/γ_N, is significantly lower than 0.5, reported elsewhere. An upturn in the heat capacity below 200 mK is also reduced compared to other studies and is well described by a Schottky anomaly and residual Sommerfeld term rather than quantum critical behaviour.

Keywords: UTe_2, unconventional superconductivity, heavy-fermion

I. INTRODUCTION

The discovery of unconventional superconductivity in the heavy-fermion paramagnet UTe_2 sparked a whirlwind of activity. Subsequent research revealed that the material possibly hosts equal spin Cooper pairs [1, 2], and lies close to a ferromagnetic quantum critical point [3]. As such, UTe_2 is related to the ferromagnetic superconductors (UGe_2 [4], URhGe [5] and UCoGe [6]), in which ferromagnetic spin fluctuations are widely believed to mediate superconductivity. This comparison may be drawn out further, as UTe_2 also exhibits field re-entrant superconductivity [7]. The unconventional nature of the superconductivity in UTe_2 has motivated the search for signatures of non-trivial topology, with one STM study [8] reporting evidence for chiral modes existing inside the superconducting gap.

Under pressure, a second superconducting transition appears [9, 10], accompanied by an almost two-fold increase in the transition temperature. Recently, a splitting of T_c has also been observed in the heat capacity at ambient pressure [11], although it is unclear whether the two splittings have a common origin. The majority of specific heat studies observe a residual Sommerfeld coefficient, γ^*, within the superconducting state [8, 9, 12], something which has been interpreted as evidence for non-unitary pairing [1]. The magnitude of this residual contribution is typically measured to be approximately half of the normal state value, γ_N, leading some studies to suggest that only one of the two spin directions is paired in the superconducting state [2]. However, the interpretation of the low temperature specific heat is controversial - with more recent lower temperature investigations reporting an upturn of C/T [13, 14]. Characterising and understanding the upturn is critical to establishing whether a residual Sommerfeld contribution is indeed present, and by extension, whether the usual entropy balance between the superconducting and normal states is maintained. Identifying the cause of the upturn is complicated by the disparate form of C/T observed by different groups [13, 14]. This raises the question - to what extent does sample quality, or composition, impact the physics?

Previously, UTe_2 single crystals have been grown either by a self-flux method or by chemical vapour transport (CVT). The self-flux method [2], with a U:Te ratio of 22:78 and centrifuging away excess Te-flux, produced lower quality samples than CVT growth. Early growths of UTe_2 by CVT started with stoichiometric U:Te atomic ratio of 1:2 [15–17], with a halogen like iodine or bromine as the transport reagent. More recent studies [1–3] instead, almost exclusively, start with a U:Te ratio of 2:3. In this study we have attempted to reproduce both of these CVT growths, and also investigated a growth for an intermediate U:Te ratio. Our energy dispersive X-ray analysis shows that the CVT element ratio modifies the stoichiometry of the crystals grown. With increasing tellurium content we see an initial increase of the superconducting transition temperature and obtain samples with the highest T_c reported to date, at ambient pressure. We find that further increasing Te content however destroys superconductivity completely. Samples with high T_c show no evidence for a double-step superconducting transition. The low temperature specific heat data are well described by a residual Sommerfeld term plus a Schottky contribution. By comparing our data with all published data we see a clear inverse correlation between T_c and γ^*/γ_N. Finally, the fact that γ^*/γ_N is significantly lower than 0.5 in our higher T_c samples argues against the interpretation that only one spin direction is paired.

II. METHODS AND RESULTS

A. Sample synthesis

Samples were grown with depleted U (AMES laboratory, electrotransported, >99.99%) that was electrochemically etched to remove surface oxide, Te (GoodFellow, >99.999% purity) and I_2 (Alfa Aesar, 99.5% purity),

which is the transport reagent for the CVT. The uranium and tellurium, ∼1 g each, were sealed in an evacuated 12 mm internal diameter quartz tube with ∼50 mg of I_2. A temperature gradient from 950 to 860°C was maintained along the 15 cm long tube for 12 days [15]. After synthesis, samples were mechanically removed from the quartz tube and washed in ethanol to dissolve residual iodine. Three growths were conducted, labelled A, B and C, with Te/U ratios given in Table I. Laue X-ray diffraction was used to orient single crystal samples. The diffraction pattern could be fully indexed with the orthorhombic structure reported in [15]. None of the room temperature diffraction patterns showed evidence for a tetragonal phase reported in [18], that is reported to be stabilised by inclusion of oxygen or elements such as germanium in [19]. Individual single crystals are identified by a letter, corresponding to the growth, and a number. In the following sections we focus mainly on samples from growth C as they show substantial differences from samples reported elsewhere.

B. Energy dispersive X-ray analysis

Energy dispersive X-ray analysis (EDX) was used to identify the composition of samples and homogeneity variations. The measurements were carried out on a Zeiss Crossbeam 550 FIB/SEM from Quorum Technologies with an accelerating potential of 10 kV. The estimate of the penetration depth for pure uranium is 0.3 µm [20].

The range of results measured by EDX are summarised in Table I for all growths. Line scans and point scans were taken over the facets of single crystal samples from each growth to characterise the variation within a sample and within the growths. These scans are used to deduce the atomic percentages of elements in a sample. One to three scans between 800 µm - 1200 µm (approximately the sample size) in length were taken over sample surfaces, for two samples from growth A and four samples from each of growths B and C. The line scans do not show a deviation in counts across the sample surface outside the standard error about the mean count. No evidence was seen for precipitates of other compositions. Though the absolute atomic ratio may be subject to systematic error, the EDX analysis should still determine relative changes of atomic ratio between the growths.

Growth	CVT Te/U at. ratio	Range of EDX Te/U at. ratio	T_c (K)
A	1.71	1.46 - 1.50	1.74
B	2.14	1.79 - 2.06	no SC
C	1.85	1.72 - 1.87	2.00

TABLE I. The different starting atomic ratios Te/U for growths A, B and C, the resulting composition measured by EDX and the superconducting transition temperature as measured by resistivity. Samples from growth B do not show a superconducting transition down to 50 mK.

The Te:U ratio for unoriented single crystals C1-C4 are shown in Table II. Sample C2 has a higher atomic ratio than other samples studied from this growth. The studied surface of this sample was curved indicating it came from a region in contact with the inner quartz tube wall, which may lead to an anomalous stoichiometry. The other samples have a spread of stoichiometry within the measurement error.

Sample	Atomic ratio Te/U
C1	1.73
C2	1.87
C3	1.76
C4	1.72

TABLE II. Measured Te/U atomic ratio in samples C1-C4. The error of each value is ±0.04.

C. Resistivity

Resistivity was measured by a 4-probe method with the contacts located on as grown flat facets with a current of 10 µA at a frequency of 37 Hz.

The low temperature resistivity of unoriented samples C5 and A1 (both single crystals ∼1 mm in dimensions), normalised to 4 K, is shown in Figure 1. From a fit to the low temperature resistivity we deduce an RRR∼10 for sample C5. Also shown in Figure 1 is a comparison with resistance data published by [1] and [11] close to T_c, which shows the higher T_c of C5 and a similar width of superconducting transition. Sample A1 has a superconducting transition at 1.74 K, closer to T_c values reported in [1] and [11] which both used a CVT atomic ratio of 2:3. A sample from growth B showed no superconductivity. Growth B crystals are the closest to 1:2 stoichiometric UTe_2. Previous work on stoichiometric crystals showed a sudden volume change at 100 K and new X-ray diffraction spots appeared slowly below 23 K [16]. We have not investigated this possibility further at the present time. In contrast, recent work on superconducting crystals with a similar T_c to growth A did not show any structural changes down to 2.7 K [21].

The resistivity of sample C5 shows a sharper and larger maximum occurring at the Kondo hybridisation crossover than crystals reported in other studies, with a maximum occurring at $T_K = 16$ K. In [1] and [2], $T_K \approx 77$ K (current $j \parallel a$ & $\parallel b$) and 50 K (current $j \parallel a$) respectively.

D. Specific Heat

The specific heat was measured for three samples from growth C, namely C5 - an unoriented single crystal - and C6 and C7 - spark-cut, oriented single crystals. As shown in Figure 2 (a), all samples exhibit similar behaviour, but with small differences at the lowest temperatures.

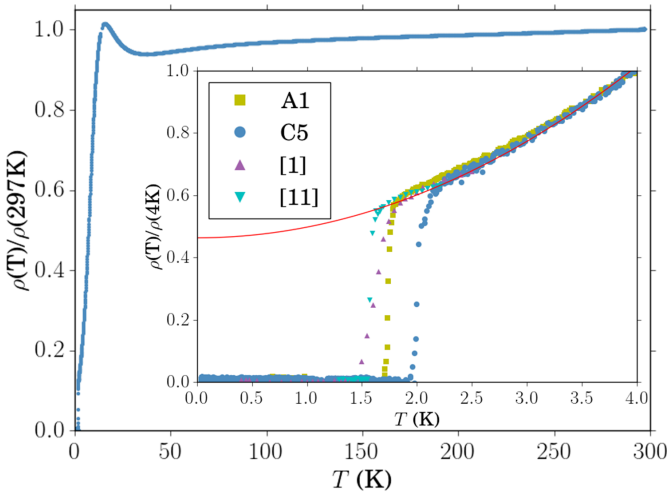

FIG. 1. Normalised resistivity of samples A1 and C5 showing a superconducting transition at 1.74 K and 2.00 K respectively (the temperature at which the resistance has fallen to 50% of its normal state value). A fit to $\rho(T) = \rho_0 + aT^2$ is shown in the inset (red line), used to extrapolate the lower temperature resistivity, giving an RRR∼10. Resistance data are also shown from [1] (original data divided by 0.0292 mΩ cm) and [11] (original data divided by 1.84 mΩ cm) for comparison in the inset. The main plot shows the normalised resistivity data for C5 up to 297 K. The Kadowaki-Woods ratio, a/γ_N^2, calculated for sample C5 is ∼100 μΩ cm mol^2 K^2 J^{-2}, similar to that reported in [1] and a similar magnitude to heavy-fermion compounds in general [22].

All data were taken with the relaxation time method, with $\Delta T \sim 0.5\%\ T$ over the full temperature range. The addenda contribution has been subtracted in all cases, and was less than 25% of the total magnitude at the lowest temperatures, falling to less than 2% above 1 K.

The function

$$\frac{C}{T} = \beta T^2 + \left[\frac{1}{2} + \frac{1}{2}\tanh\left(\frac{T-T_c}{\delta}\right)\right]\gamma_N - \left[\frac{1}{2}\tanh\left(\frac{T-T_c}{\delta}\right) - \frac{1}{2}\right](\alpha T^\lambda + \gamma^*) + \frac{A_{sch}}{T^3} \quad (1)$$

was used to describe the data. The function is purely phenomenological, but useful for comparing different sets of data, and extracting the parameters, T_c, ΔT_c (the 10-90% transition width, $\Delta T_c = 2.2\delta$) and γ_N (the normal state Sommerfeld coefficient). The expression also provides an estimate of the phonon contribution (βT^2) that can then be subtracted to give the electronic heat capacity. In addition, terms have been included to account for the previously reported unconventional superconductivity (αT^λ), residual Sommerfeld coefficient (γ^*) and Schottky anomaly (A_{sch}), all of which will be discussed below. Shown in Figure 2 (b) is the fit for sample C6.

Figure 2 (c) shows similar fits to the zero-field specific heat data from previous studies [2, 12–14]. The parameters extracted from these fits are collated in Table III. The data from [1, 8, 9] were also analysed in a similar way, but have been omitted from the figure for clarity. From Figure 2 (c) (and Table III), three things are immediately obvious: our growth C samples (i) have the largest T_c, (ii) show the largest jump at the superconducting transition, and (iii) have the smallest Sommerfeld coefficient. Within the superconducting state, the data from our samples lie on a separate curve to all the others. Note, in calculating the specific heat for our samples, we have taken the average stoichiometry from the EDX measurements ($UTe_{1.77}$). Therefore, in order to demonstrate that the observed difference in superconducting behaviour is not an artefact of this normalisation, we have also compared the data after normalising to the normal state Sommerfeld coefficient. This is shown in the inset of Figure 2 (c). Finally, we have analysed those data points at the transition using a modified form of the 'large pulse method' [23], and see no evidence for a split transition.

We now consider the low temperature behaviour, which, as shown in Figure 2 (d), varies between different investigations. Previous specific heat studies can be divided into two categories:

(A) Those which do not measure low enough in temperature to see an upturn [1, 8, 9, 12]. The majority fit the lowest temperature data using $C/T = \alpha T^2 + \gamma^*$, which leads to the inevitable conclusion of a residual contribution γ^*.

(B) Those which do go low enough in temperature to see an upturn [2, 13, 14]. In one study [13], this behaviour is described by a 'divergent quantum-critical contribution'

$$\frac{C}{T} = \alpha T^2 + A_{div} T^{-m}, \quad (2)$$

where $m \sim 0.33$, such that a residual term γ^* is unnecessary.

Our data falls into the second category, in that we do see an upturn, however we find this upturn is modelled better using

$$\frac{C}{T} = \alpha T^2 + \gamma^* + \frac{A_{sch}}{T^3}. \quad (3)$$

Importantly, we find that in order to fit the data from samples C5, C6 and C7 adequately, we also require a residual term γ^*.

Shown in Figure 2 (d) is a comparison of all those data sets which extend to low enough temperature to see an upturn. Also shown are fits to Equation 2 (with $0 < m < 1$) and Equation 3, only including the low temperature ($T < 1$ K) data. Whilst the data from [13] are clearly better described by the quantum critical scenario of Equation 2, in all the other cases, the upturn appears too sharp, and is therefore better fit by the Schottky model of Equation 3. Again, for an adequate

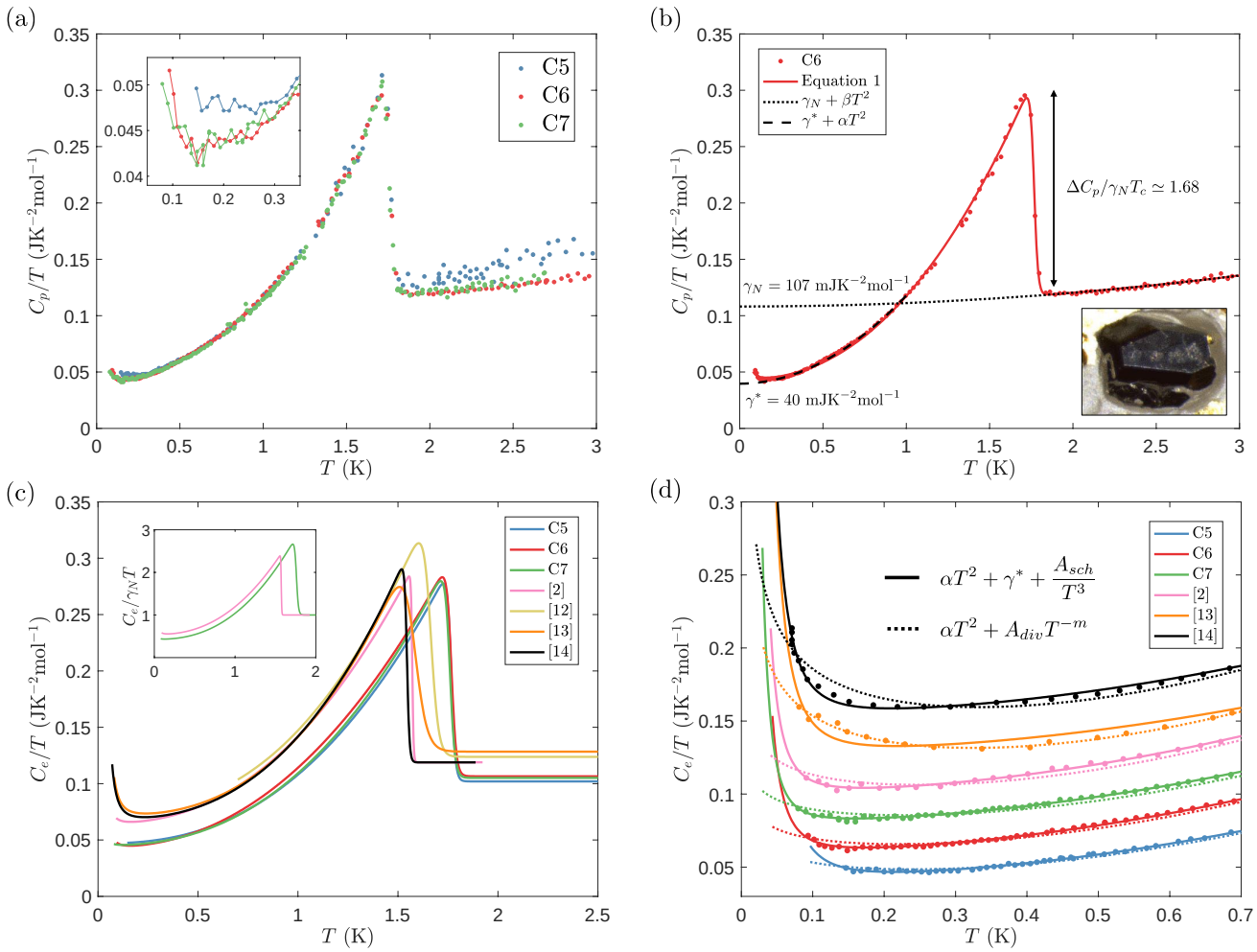

FIG. 2. (a) Zero-field specific heat capacity as a function of temperature for samples C5, C6 and C7. The inset shows the low temperature behaviour. (b) Sample C6 specific heat data and fit to Equation 1 (solid line). Also shown is the low temperature (< 1 K) fit to Equation 3 minus the Schottky contribution (dashed line), which gives the residual term γ^*. The inset shows a microscope image of sample C6. (c) Fits of the data from samples C5, C6 and C7, as well as the zero-field specific heat from previous studies, to Equation 1, with the phonon contribution subtracted. The extracted parameters are listed for comparison in Table III. The inset shows a comparison of sample C7 to that from [2], both normalised to their respective normal state Sommerfeld coefficient. (d) Low temperature fits to a Schottky model (solid lines) and a quantum critical model (dotted lines), described in the text. The data sets have been offset for clarity.

	C5	C6	C7	[1]	[2]	[2]	[8]	[9]	[12]	[13]	[14]
T_c (K)	1.77	1.77	1.76	1.64	1.57	1.46	1.53	1.45	1.66	1.58	1.54
ΔT_c (K)	0.05	0.05	0.05	0.05	0.02	0.05	0.07	0.04	0.06	0.12	0.03
γ_N (mJK^{-2}mol^{-1})	102	107	105	112	119	122	132	122	124	128	119
$\Delta C/\gamma_N T_c$	1.86	1.68	1.81	1.41	1.39	1.11	1.26	1.15	1.63	1.16	1.58
A_{sch} (μJKmol^{-1})	-	71 ± 23	47 ± 21	-	78 ± 29	-	-	-	-	*	191 ± 18
γ^* (mJK^{-2}mol^{-1})	42	40	40	55	60	70	59	68	52	68	63
γ^*/γ_N	0.41	0.37	0.38	0.46	0.51	0.57	0.45	0.55	0.42	0.53	0.53

TABLE III. Parameters from fits to Equations 1 and 3 (see Figures 2 (c) and 2 (d)). The Schottky coefficient (A_{sch}) is only listed for those data sets which extend below 100 mK. The error corresponds to the A_{sch} at which χ^2 has reached twice its minimum value. * indicates the fit was not appropriate, as shown in Figure 2 (d).

fit, all these data sets require the inclusion of a residual term γ^*. As is shown in Figure 2 (b), the value of γ^* may be extracted by subtracting the Schottky contribution and then extrapolating to zero temperature - this residual term has been included in Table III. Also included is the Schottky coefficient (A_{sch}) and the ratio γ^*/γ_N. As shown in Figure 3, this ratio appears to be negatively correlated with both T_c and the superconducting jump, $\Delta C/\gamma_N T_c$. In line with this, our growth C samples exhibit the smallest γ^*/γ_N of any study. Finally, it is worth noting that, in all cases, the goodness of the T^2 fit (Equation 3) is taken to be evidence for point nodes in the superconducting gap.

III. DISCUSSION

We have demonstrated that the superconducting properties of uranium telluride vary as a function of tellurium content. By varying the ratio of elements present in the CVT synthesis, we were able to grow samples which exhibit similar properties to the majority of previous studies [1, 2] (growth A), as well as samples which show no superconductivity (growth B). Furthermore, we have demonstrated that, for an intermediate starting ratio (growth C), the superconducting transition temperature, and the specific heat jump at this transition, are enhanced beyond any values observed previously.

The form of the specific heat is similar to the majority of other studies, and exhibits a residual term as $T \to 0$ K. One previous study instead found what they describe as a quantum critical divergence [13]. This opens up the interesting possibility that the material is being tuned about a ferromagnetic quantum critical point. However, as is clear from Table III, the value of T_c observed in [13] is not near an extremum. This argues against interpreting the low temperature specific heat data of this one study as evidence for quantum critical fluctuations. Further, no such behaviour was observed in samples with almost the same T_c, and sharper transitions [2, 14]. The rather broad superconducting transition possibly suggests a range of stoichiometry. The presence of two distinct composition ratios could also explain the double transition later reported in [11].

The low temperature specific heat exhibits a pronounced upturn at the lowest temperature. For the majority of studies, this upturn is adequately fit with a Schottky-type T^{-3} term. However, as is clear from Figure 2 (d), there is significant variation between samples, even those which exhibit similar behaviour close to T_c ([2] and [14]). Such a contribution can arise from the interaction of a nuclear quadrupole moment with a crystalline electric field gradient [24]. In this compound, ^{235}U is the only sufficiently abundant isotope to possess a quadrupole moment. Assuming an abundance of 0.2 % (for depleted uranium, as in our samples), the measured Schottky coefficients correspond to an energy splitting of approximately 50 mK, where $\Delta E = |E_{Q\ \pm 7/2} - E_{Q\ \pm 1/2}|$ [25, 26]. This value is in the range observed in other materials [27]. For natural uranium, the Schottky term would be expected to be 3-4 times larger. Additionally, there may be a contribution from defects, whose concentration could vary between samples.

We now briefly discuss the observed discrepancy between the temperature of the superconducting transition in resistivity (2.00 K) and specific heat (1.77 K). A smaller difference has also been observed in other investigations [2, 13]. Given the dependence of the superconducting transition temperature on composition, this may be explained if a part of the sample - such as a particular surface - has a slightly different stoichiometry compared to the bulk. Based on our EDX data, this would be consistent with a higher tellurium content of surfaces grown in contact with the inner quartz tube wall. This suggests that, although our samples already have the highest bulk superconducting transition temperature to date, bulk samples with T_c as high as 2 K may be possible with increased tellurium content, before reaching the value at which superconductivity is suppressed.

Finally, we draw some conclusions from a comparison of all specific heat studies (Table III). As shown in Figure 3 (a), T_c decreases with increasing γ^*/γ_N. From our own data, going from left to right in Figure 3 (a) corresponds to increasing Te content, although there is no published data on the actual Te content for those crystals grown and studied by others. The jump in the specific heat ($\Delta C/\gamma_N T_c$) also increases with T_c. The simplest way to link this jump to the ratio γ^*/γ_N is to consider that a fraction of the sample is superconducting, while a fraction remains in the normal state. This implies

$$\frac{\Delta C}{\gamma_N T_c} = \left(1 - \frac{\gamma^*}{\gamma_N}\right) a, \tag{4}$$

where $a = 1.43$ for BCS superconductivity, with higher values possible for strong coupling. As shown in Figure 3 (b), the existing data is adequately described by this relation with $a = 2.76$, which would indicate strong coupling. This analysis is clearly over-simplistic, and more information on the origin of superconductivity, γ^* and the metallurgy of UTe_2 are required to make further progress.

Despite this, we have clearly demonstrated that the superconducting properties of uranium telluride depend critically on stoichiometry, and specifically on tellurium content. Exactly how the Te deficiency is incorporated in the crystals of UTe_2 is unknown, but this has to be consistent with the sharp X-ray Laue diffraction patterns we observe, sharp superconducting heat capacity transitions and absence of precipitates in the EDX studies. For example, the Te deficiency could be linked with planar stacking faults or point-like defects. Unconventional superconductivity is known to be suppressed at many types of surface [28], so planar defects might result in a residual density of states, located close to defect planes. Resonant scattering from point-like defects is known to result in a residual normal-state-like density of states, localised in

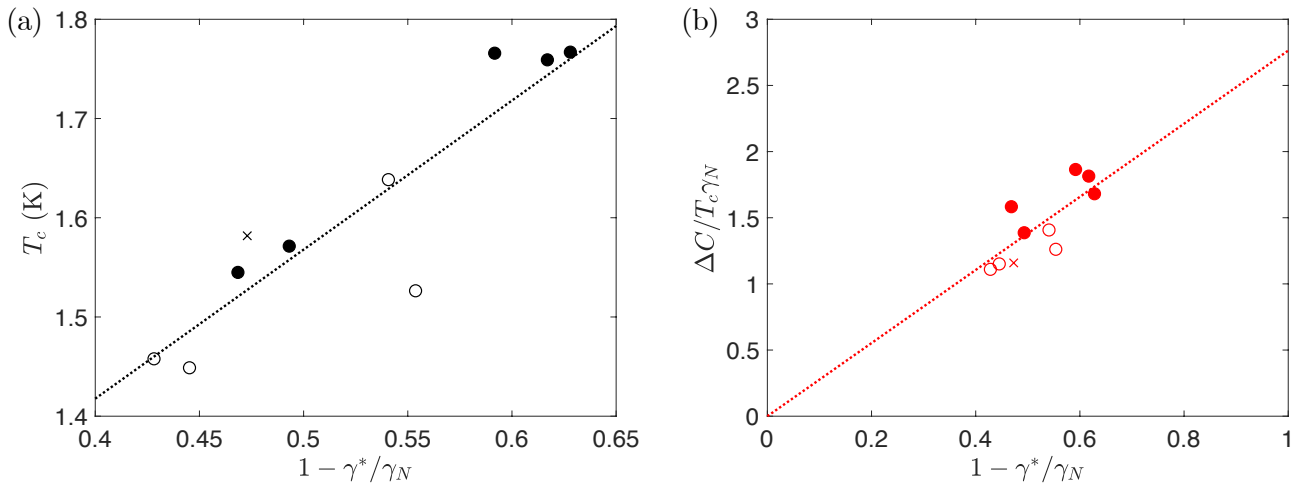

FIG. 3. The dependence of (a) the superconducting transition temperature and (b) the normalised heat capacity jump on $1-\gamma^*/\gamma_N$, where γ^*/γ_N is the ratio of residual and normal state Sommerfeld heat capacity coefficients. Data have been taken from Table III. An open (filled) point implies the lowest temperature measured was above (below) 150 mK. Crosses represent the data from [13].

reciprocal space [29]. The density of defects would in both cases also lead to a reduction of the transition temperature. This correlation between T_c and γ^* has also been observed in other unconventional superconductors [30, 31]. For the superconducting transition to remain sharp the defect density would have to be uniform over length scales larger than the coherence length. What is perhaps more surprising is that for Te content above a critical threshold, superconductivity is suppressed completely. This suggests either the presence of an as yet unidentified competing phase or that Te deficiency plays some additional role in bringing about the superconductivity. The previous observation of a low temperature structural change in the stoichiometric material [16], not seen in superconducting samples [21], may be relevant to this.

We wish to gratefully acknowledge funding from the UK EPSRC, grant numbers EP/R013004/1, EP/P013686/1 and EP/L015110/1. The authors declare no competing interests.

[1] S. Ran *et al.*, Science **365**, 684 (2019).
[2] D. Aoki *et al.*, JPSJ **88**, 43702 (2019).
[3] S. Sundar *et al.*, Phys. Rev. B **100**, 140502 (2019).
[4] S. S. Saxena *et al.*, Nature **406**, 587 (2000).
[5] F. Lévy *et al.*, Science **309**, 1343 LP (2005).
[6] N. T. Huy *et al.*, Phys. Rev. Lett. **99**, 67006 (2007).
[7] S. Ran *et al.*, Nature Physics **15**, 1250 (2019).
[8] L. Jiao *et al.*, Nature **579**, 523 (2020).
[9] D. Braithwaite *et al.*, Commun. Phys. **2**, 147 (2019).
[10] S. Ran *et al.*, Phys. Rev. B **101**, 140503 (2020).
[11] I. M. Hayes *et al.*, arXiv:2002.02539.
[12] S. Imajo *et al.*, JPSJ **88**, 83705 (2019).
[13] T. Metz *et al.*, Phys. Rev. B **100**, 220504 (2019).
[14] S. Kittaka *et al.*, arXiv:2002.06385.
[15] S. Ikeda *et al.*, JPSJ **75**, 116 (2006).
[16] K. Stöwe, J. Solid State Chem. **127**, 202 (1996).
[17] W. Suski, J. Solid State Chem. **7**, 385 (1973).
[18] A. Haneveld and F. Jellinek, J Less Common Met **18**, 123 (1969).
[19] A. K. Haneveld and F. Jellinek, J Less Common Met **21**, 45 (1970).
[20] K. Kanaya and S. Okayama, J. Phys. D **5**, 43 (1972).
[21] V. Hutanu *et al.*, Acta Crystallogr. B **76**, 137 (2020).
[22] A. C. Jacko *et al.*, Nature Physics **5**, 422 (2009).
[23] G. R. Stewart, Rev. Sci. **54**, 1 (1983).
[24] N. E. Phillips, Phys. Rev. **118**, 644 (1960).
[25] D. Bloch *et al.*, C. R. Acad. Sci. Paris **275**, 601 (1972).
[26] B. H. Suits, in *Handbook of Applied Solid State Spectroscopy* (2006).
[27] K. Ikushima *et al.*, Phys. Rev. B **63**, 104404 (2001).
[28] D. F. Agterberg and M. B. Walker, Phys. Rev. B **53**, 3516 (1996).
[29] P. J. Hirschfeld *et al.*, Phys. Rev. B **37**, 83 (1988).
[30] R. A. Fisher *et al.*, Phys. Rev. Lett. **62**, 1411 (1989).
[31] M. A. Tanatar *et al.*, Phys. Rev. Lett. **95**, 067002 (2005).